CHARACTERISATION OF SPH NOISE
IN SIMULATIONS OF PROTOPLANETARY DISCS

S. E. Arena[1], J.-F. Gonzalez[1] and E. Crespe[1]

Abstract.   We have started a characterization of the noise in SPH (Smoothed Particle Hydrodynamics) simulations of the gas component of protoplanetary discs. The main goal is the determination of the properties of the fluctuating velocity field in order to compare them to those proper both to standard incompressible Kolmogorov turbulence and to compressible supersonic turbulence. A controlled fluctuating velocity field with turbulence-like properties is very important in the context of the theories of pre-planetesimal formation where the dynamics of dust, driven by that of the gas, is the crucial point.

Keywords: protoplanetary discs, turbulence, numerical simulations

1   Introduction

While the general picture of planet formation is rather well understood, the early phase leading from mm/cm-sized dust grains to the formation of km-sized pre-planetesimals is still highly debated.

The growth of pre-planetesimals is believed to develop in the discs around Classical T Tauri stars. These discs are usually called protoplanetary discs (abbreviated in PPD) and composed mainly of gas in quasi-keplerian rotation around the central star. Only a small fraction of the total mass of the discs (about 1%-2%) is made of dust grains, which are the seeds of pre-planetesimals. Dust grains are coupled to the gas at different degrees of strength depending on their size. Two main mechanisms are the direct consequence of this coupling: radial drift and vertical settling. In addition the action of turbulence on the dynamics of dust is expected to be of relevant importance. It can have two competing effects, mediated by gas drag: stirring up and diffusing dust particles, preventing their agglomeration; or trapping them inside eddies, favoring their agglomeration. Here we focus on the mechanism of turbulence.

Current observations have not yet reached the resolution necessary to directly detect turbulence and study its effects. However, the measured values of mass accretion rates onto the central star ($\dot{M}_0 \approx 10^{-8}$ $M_\odot$/yr; Hartmann et al. 1998; Andrews et al. 2009) and the estimated life time of discs (around 10^7 yr; see e.g. Armitage 2007) imply a kinematic viscosity much larger than the molecular viscosity in PPD (20 m^{2}s^{-1}; see e.g. Armitage 2007). Shakura & Sunyaev (1973) noted that turbulence can provide an effective viscosity able to justify these data.

Given the complex interplay between dust and gas, the problem can be only addressed by numerical simulations. In this work we focus mainly on the study of the fluctuating velocity field of gaseous discs evolved by means of Smoothed Particle Hydrodynamics (SPH) simulations. Our aim is to clarify if the numerical noise intrinsically present in SPH simulations of accretion discs can mimic the effects of turbulence and to what extent. A set of SPH simulations of a gaseous disc with different numerical and physical parameters has been performed. For each simulated disc we have studied both the magnitude and the structure of the fluctuations present in the velocity field. The resulting properties of such fluctuations have been compared to the typical behaviour of turbulence and to results from grid based simulations available in the literature.

---

[1] Université de Lyon, Lyon, F-69003, France; Université Lyon 1, Observatoire de Lyon, 9 avenue Charles André , Saint-Genis Laval, F-69230, France; CNRS, UMR 5574, Centre de Recherche Astrophysique de Lyon; École Normale Supérieure de Lyon, Lyon, F-69007, France

2   The disc model, the code and the simulations

The reference disc model   A Classical T Tauri disc of mass $M_{\mathrm{disc}} = 0.01\, M_{\mathrm{star}}$ orbiting around a one solar mass star ($M_{\mathrm{star}} = M_\odot$) is considered. It extends from 20 to 400 AU, it is characterized by a surface density radial profile given by $\Sigma(r) = \Sigma_0 (r/r_0)^{-p}$ and it is locally isothermal with a sound speed radial profile $c_s(r)$ given by $c_s^2(r) = c_{s_0}^2 (r/r_0)^{-q}$. The semi-thickness H of the disc is related to the sound speed and to the angular velocity Ω by $H(r) = c_s(r)/\Omega(r)$. Note that the sound speed coefficient c_{s_0} and the sound speed exponent $q/2$ determine respectively the semi-thickness of the disc and its radial dependence $H(r) \propto r^{(3-q)/2}$.

The reference values we adopt in the following are $p = 3/2$ and $q = 3/4$ typical of the Minimum Mass Solar Nebula. The disc is slightly flared with $H(r)/r = 0.05$ at $r = 100$ AU. The evolution of the disc is followed for about 10 orbits (at 100 AU) after numerical thermalisation has been reached.

The code   We use the two-phase SPH code described in Barrière-Fouchet et al. (2005). The two phases represent gas and dust that interact via aerodynamic drag. The gas is described by Euler equations and artificial viscosity is used to model physical viscosity as described in Meglicki et al. (1993). Here we consider only the gas phase because we are interested in the modeling of gas turbulence. The smoothing length h is variable and is derived from the density ρ: $h = h_0 (\rho_0/\rho)^{1/3}$, in order to guarantee a roughly constant number of neighbours. The kernel is a cubic-spline.

The Monaghan & Gingold (1983) artificial viscosity is implemented. Here we recall this formulation because the two parameters α and β are relevant for the following study: $\Pi_{ij} = \left(-\alpha \bar{c}_{ij}\mu_{ij} + \beta\mu_{ij}^2\right)/\bar{\rho}_{ij}$ when $\mathbf{v}_{ij} \cdot \mathbf{r}_{ij} < 0$ and zero otherwise; $\mathbf{r}_{ij}$ and $\mathbf{v}_{ij}$ are respectively the relative distance and relative velocity. The overlined quantities are averages between particle i and its neighbouring particle j: $\bar{c}_{ij} = (c_i + c_j)/2$, $\bar{\rho}_{ij} = (\rho_i + \rho_j)/2$, $\bar{h}_{ij} = (h_i + h_j)/2$. Finally, $\mu_{ij} = \bar{h}_{ij}\mathbf{v}_{ij} \cdot \mathbf{r}_{ij}/(\mathbf{r}_{ij}^2 + \bar{h}_{ij}^2\eta^2)$, with $\eta^2 = 10^{-2}$.

The internal units of the code are set in order to have the gravitational constant $G=1$ and are: 1 $M_\odot$ for mass, 100 AU for length and $10^3/2\pi$ yr for the time. In the following, all the results are expressed in code units.

The simulations   We have performed two groups of simulations. Simulations in the first group are identified by the AV name followed by the relative number: the two Artificial Viscosity parameters α and β are changed. Simulations from AV1 to AV5 are characterized by $\alpha = 0.1$ and $\beta = 0, 0.2, 0.5, 2, 10$ respectively. Simulations AV6 and AV7 have $(\alpha, \beta) = (1,0)$ and $(\alpha, \beta) = (1,2)$ respectively. Simulations AV8 has $(\alpha, \beta) = (0,10)$ and AV10 has $(\alpha, \beta) = (5,0)$. All the other parameters are those of the reference model. In the second group we have two simulations: DP1 where the parameter of the Disc Profile of the sound speed is changed in $q = 1.5$ and DS1 where, in addition, the coefficient of the Disc Sound speed is increased at $c_{s_0} = 0.1$. For simulations in this group we have taken the standard values for the artificial viscosity parameters: $(\alpha, \beta) = (1,2)$.

All discs are sampled by $2 \cdot 10^5$ particles and initially evolved for about 9 orbits (at 100 AU) in order to reach numerical thermalisation. The face-on and edge-on view of the surface density profile of four of the simulated discs are displayed in Fig. 1.
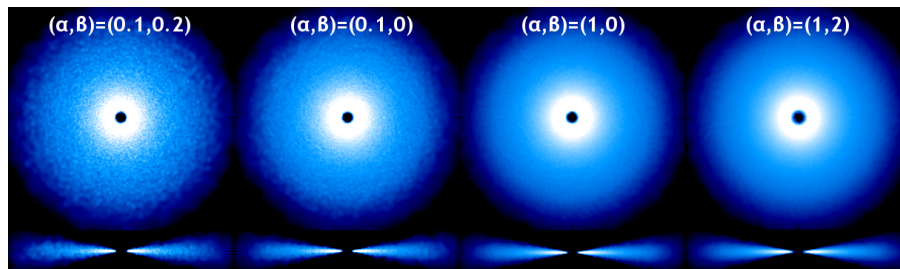
Fig. 1. The simulations: face-on and edge-on view of the surface density for simulations AV1, AV2, AV6, AV7 (from left to right).

3   Magnitude of SPH noise

A. Central mass accretion rate and turbulent viscosity estimated by $\alpha_{\mathbf{ss}}$ In accretion disc theory, the observed central mass accretion rate $\dot{M}_0$ is connected to the turbulent viscosity coefficient ν_{T}. The latter is

parametrised by the dimensionless quantity α_{ss} by means of the scale height and the sound speed: $\nu_T = \alpha_{ss} c_s H$ (Shakura & Sunyaev 1973). For protoplanetary discs $\dot{M}_0 \approx 10^{-8}$ M$_\odot$/yr and $\alpha_{ss} \approx 10^{-2}$ (Hartmann et al. 1998; King et al. 2007). The central mass accretion rate measured in our simulations is displayed in the left plot of Fig. 2: for all simulations we found values consistent with the reference values from observations. In addition, the plot shows that larger artificial viscosity parameters lead to larger accretion rates onto the central star.

Following Fromang & Nelson (2006) we computed the α_{ss} parameter starting from Reynolds stress: $\alpha_{RS} = \langle u_r u_\theta \rangle / \langle P/\rho \rangle$, where P and ρ are respectively the pressure and density of the gas, u_r and u_θ are the velocity fluctuations in the radial and azimuthal directions and the symbol $\langle \cdot \rangle$ represents average quantities. The result displayed in the right plot of Fig. 2 shows that the behaviour of α_{RS} is very sensitive to the numerical noise. For sufficiently large α and β (e.g. simulations AV7 and AV9) the modulus of α_{RS} correlates with the central mass accretion rate and is in agreement with the value of 10^{-3} found by Fromang & Nelson (2006). In the other cases, the value of α or β is too low and the consequent noise breaks this correlation. The negative values of α_{RS} are due to the dominant outward flow in the region around the midplane, which characterizes the mechanism of meridional circulation present in these models.

A general view of the flow in the disc is given by colour plots of the radial velocity field in face-on sections of the discs. In Fig. 3 a transition from a chaotic to a more regular flow structure is visible comparing simulation AV1 with AV7.
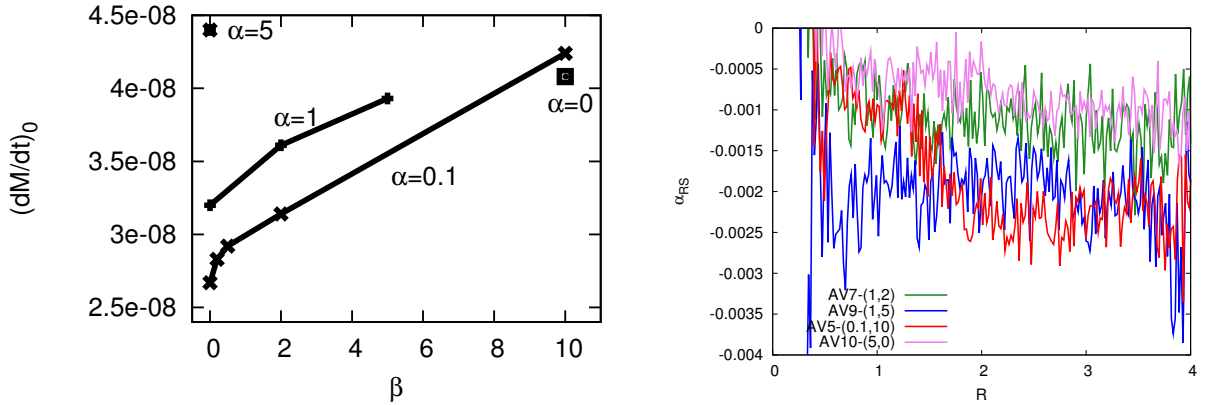
Fig. 2. Magnitude of SPH noise. **Left**: central mass accretion rate $\dot{M}_0$ in unit of M$_\odot$/yr. **Right**: radial profile of α_{RS}, which gives an estimate of α_{ss} based on Reynolds stress.

B. Vertical diffusion coefficient   Following Fromang & Papaloizou (2006) we computed the turbulent diffusion coefficient D_T starting from the vertical velocity correlation function $S_{zz}(t) = \langle v_z[z(z_0,t),t]v_z(z_0,0)\rangle$: $D_T(t) = \int_0^t S_{zz}(t')\mathrm{d}t'$, where the zero refers to quantities at the initial time $t = 0$, z is the vertical position of each particle and v_z the vertical component of velocity.

The evolution with time of the diffusion coefficient D_T (in units of $c_s H$), measured at the intermediate radial position $r = 1.82$, is shown in Fig. 4 for all simulations. Results at different locations are qualitatively similar. The diffusive mechanism is correctly represented by large artificial viscosity parameters (α, β). More viscous and less extended discs are less diffusive. For the usually adopted combinations of parameters $(\alpha, \beta) = (1, 2)$, $D_T/(c_s H) \approx 5 \cdot 10^{-3}$ is in agreement with the value found by Fromang & Papaloizou (2006) in their MHD local shearing box stratified simulations.

4   Structure of SPH noise

Power spectrum   Since the system is not homogeneous, we compute the power spectrum for each component of velocity along a ring located at different radii from the central star and at several altitudes: $P(k) = |\hat{u}_i(k)|^2$, where $\hat{u}_i(k)$ is the Fourier transform of the i component of the velocity fluctuation vector. In the two reference cases considered, the power spectrum is given by a power law: $P(k) \sim k^\delta$, with $\delta = -5/3$ in the incompressible
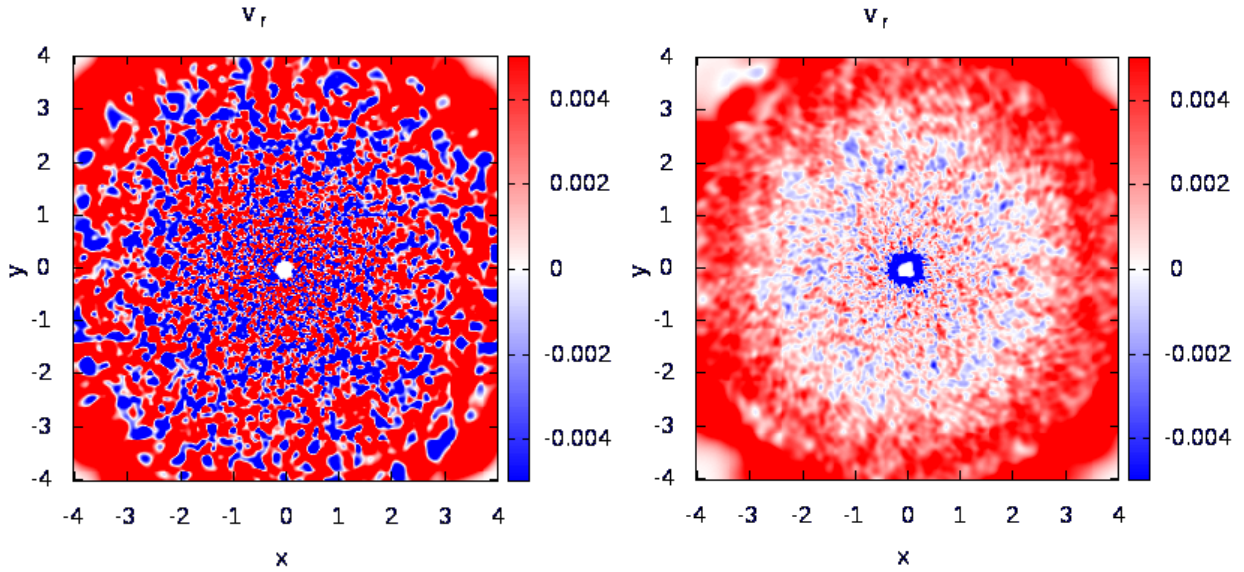
Fig. 3. The face-on view of the cross section of the radial velocity field of the disc for simulation AV1 (left) and AV7 (right) shows the transition from a chaotic to an ordered and more regular flow.
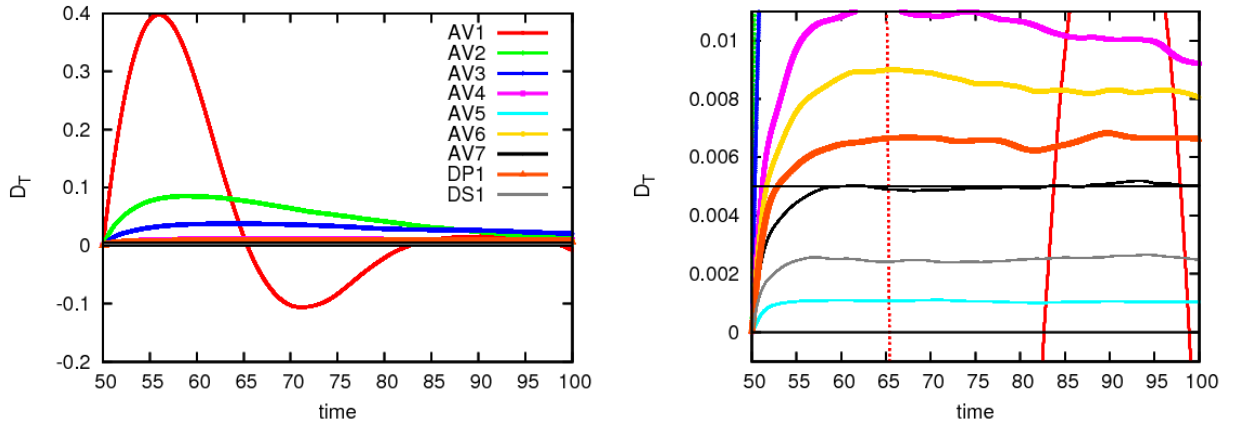
Fig. 4. Magnitude of SPH noise. The turbulent diffusion coefficient $D_T(t)$. The right panel represents an enlargement of the y-axis in order to better distinguish the curves that refers to simulations from AV4 to DS1.

Kolmogorov (1941) case and $\delta \approx -1.75, -2$ in the compressible supersonic case (e.g. see Price & Federrath 2010).

Figure 5 shows that when the artificial viscosity term is weak (low α and low β) a clear cascade is not identified (see left panel). However, larger (α, β) pairs lead to a cascade that is limited by the vertical extension of the disc at small wave numbers and by the resolution at high wave numbers. The exponent of the observed cascade is close to that of the compressible supersonic case mainly for the radial component for intermediate values of the artificial viscosity parameters (see middle panel), in the other cases, azimuthal and vertical components and increasing artificial viscosity, it tends to approach that of the Kolmogorov case (see right panel).

An increase in resolution, artificial viscosity and sound speed leads to more extended cascades. The features observed for the power spectrum are qualitatively preserved at different radial and vertical positions inside the disc.

Intermittency Highly turbulent flow are characterized by *intermittency*. This feature is highlighted by the exponent of the structure function and higher order moments of probability distribution functions (PDF) of several quantities such as density and velocity. We have analysed the 3rd (skewness S) and the 4th (kurto-
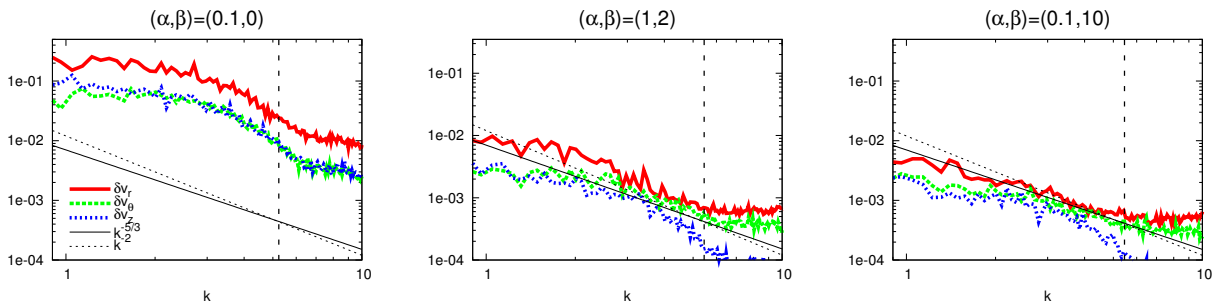
Fig. 5. Structure of SPH noise. Power Spectrum of velocity fluctuations: radial, azimuthal and vertical components are represented with solid red, dashed green and blue dotted lines respectively. The vertical long dashed line represents the resolution limit. The solid and the dotted black lines represent the Kolmogorov and the $\delta = -2$ slope of the power spectrum, respectively.

sis K) moment: no significant deviation from the gaussian values has been observed, indicating absence of intermittency.

5   Conclusions

The noise in SPH simulations, called here SPH noise, can be considered as the numerical noise filtered by the model chosen for the implementation of artificial viscosity. SPH noise produces a fluctuating field that depends both qualitatively and quantitatively on the artificial viscosity term.

Simulations with significantly large (α, β) parameters, among those considered, have given encouraging results. In this case, the Monaghan & Gingold (1983) artificial viscosity implementation partially mimics the effects of a physical turbulent viscosity: an energy cascade is present, accretion and turbulent diffusion are reproduced (but inversely related); however intermittency is not present.

Further investigation is necessary before studying the effect of highly turbulent gas on the dynamics of dust grains.

References

Andrews, S. M., Wilner, D. J., Hughes, A. M., Qi, C., & Dullemond, C. P. 2009, ApJ, 700, 1502

Armitage, P. J. 2007, ArXiv Astrophysics e-prints, arXiv:astro-ph/0701485

Barrière-Fouchet, L., Gonzalez, J., Murray, J. R., Humble, R. J., & Maddison, S. T. 2005, A&A, 443, 185

Fromang, S. & Nelson, R. P. 2006, A&A, 457, 343

Fromang, S. & Papaloizou, J. 2006, A&A, 452, 751

Hartmann, L., Calvet, N., Gullbring, E., & D'Alessio, P. 1998, ApJ, 495, 385

King, A. R., Pringle, J. E., & Livio, M. 2007, MNRAS, 376, 1740

Kolmogorov, A. 1941, Akademiia Nauk SSSR Doklady, 30, 301

Meglicki, Z., Wickramasinghe, D., & Bicknell, G. V. 1993, MNRAS, 264, 691

Monaghan, J. & Gingold, R. 1983, Journal of Computational Physics, 52, 374

Price, D. J. 2007, PASA, 24, 159

Price, D. J. & Federrath, C. 2010, MNRAS, 406, 1659

Shakura, N. I. & Sunyaev, R. A. 1973, in IAU Symposium, Vol. 55, X- and Gamma-Ray Astronomy, ed. H. Bradt & R. Giacconi, 155–+